THE GEOLOGY OF ROTHSCHILD ISLAND, NORTH-WEST ALEXANDER ISLAND

By B. W. CARE

ABSTRACT. Sedimentary, volcanic and plutonic rocks from Rothschild Island are described for the first time. Steeply dipping but relatively undeformed mudstones, greywackes, mud-flake breccias and pebble-conglomerates are believed to be equivalent to the (?) Permian–Triassic LeMay Formation of northern and central Alexander Island. A period of hornblende-andesite dyke intrusion was followed by the emplacement of six (?) Tertiary plutons of predominantly granodioritic composition and by later injection of quartz-plagioclase-porphyry and intermediate dykes. Two outcrops of bedded palagonite-tuffs, lapilli-tuffs and lapillistones, intruded by olivine-basalt dykes in the south-east of the island, represent new discoveries within the wide belt of Cenozoic volcanic rocks extending across western Antarctica. Twenty-five modal analyses and ten geochemical analyses are presented. The plutonic rocks show comparable trends to the calc-alkali suites of the Antarctic Peninsula, and the geochronological and genetic relationships between the plutonic and hypabyssal rocks are described in terms of their inter-element ratios. A high K_2O content indicates an apparent reversal in the east–west decrease of potash values previously described from Graham Land and may reflect an increased depth to the Benioff Zone. Structural evidence for two periods of folding is given and the difference in trends of fold axes compared to those of northern Alexander Island is explained in terms of movement within the cataclastic belt situated along the west coast of Alexander Island.

THE identity of Rothschild Island remained unresolved for more than a century following the first sighting by Thaddeus von Bellingshausen in January 1821. During this voyage past the north-west coast of Alexander Island, Bellingshausen described three similar high topographic features separated by two gaps (Debenham, 1945). The most westerly of these can now be identified as Mirnyy Peak on Rothschild Island, the others being St. George Peak in the Havre Mountains and Mount Bayonne in the Rouen Mountains, with the intervening divides of Lazarev Bay and Russian Gap. Although the feature was seen from a closer distance by Dr J.-B. Charcot during the French Deuxième Expédition au Pole Sud, 1908–10, and given the name "Ile E. de Rothschild", the descriptions "Mount Rothschild" and "Cape Rothschild" were proposed as a result of misleading aerial observations made during later expeditions, implying that the feature was part of the mainland of Alexander Island. However, its insularity was finally realized when a flight from East Base of the United States Antarctic Service Expedition (USASE) in November 1940 discovered . . . "a strait 6–10 miles wide . . ." separating the feature from the mainland (Black, 1945) and, after verification of this sighting by the Ronne Antarctic Research Expedition (RARE), 1946–1948, the name Rothschild Island was adopted.

The island was first visited in January 1976 when a British Antarctic Survey team was flown in to establish a topographical survey station but it remained unexplored until the author, accompanied by a general assistant, spent 5 weeks geologically mapping the island during the austral summer of 1976–77.

PHYSIOGRAPHY

Rothschild Island is situated between lat. 69°25′ and 69°45′S, and long. 72° and 73°W, off the north-west coast of Alexander Island (Fig. 1) and has an area of approximately 700 km². The island is separated from Alexander Island by the 10–25 km wide Lazarev Bay, which terminates in the Wilkins Ice Shelf at its southern end, and is ice-bound for much of the summer. Coastal ice cliffs exceeding 30 m in height fringe the western and northern margins of the island but are breached in the east by small rocky headlands and islets, and a small glacier flowing into Lazarev Bay; the southern coast of Rothschild Island merges almost imperceptibly with the Wilkins Ice Shelf, which connects it to the mainland in the east and to Charcot Island, 75 km to the west.

A central range of snow-capped peaks (including *c.* 1 500 m Enigma Peak) extending 20 km east–west across the island separates the northern snowfield (350–400 m maximum elevation)

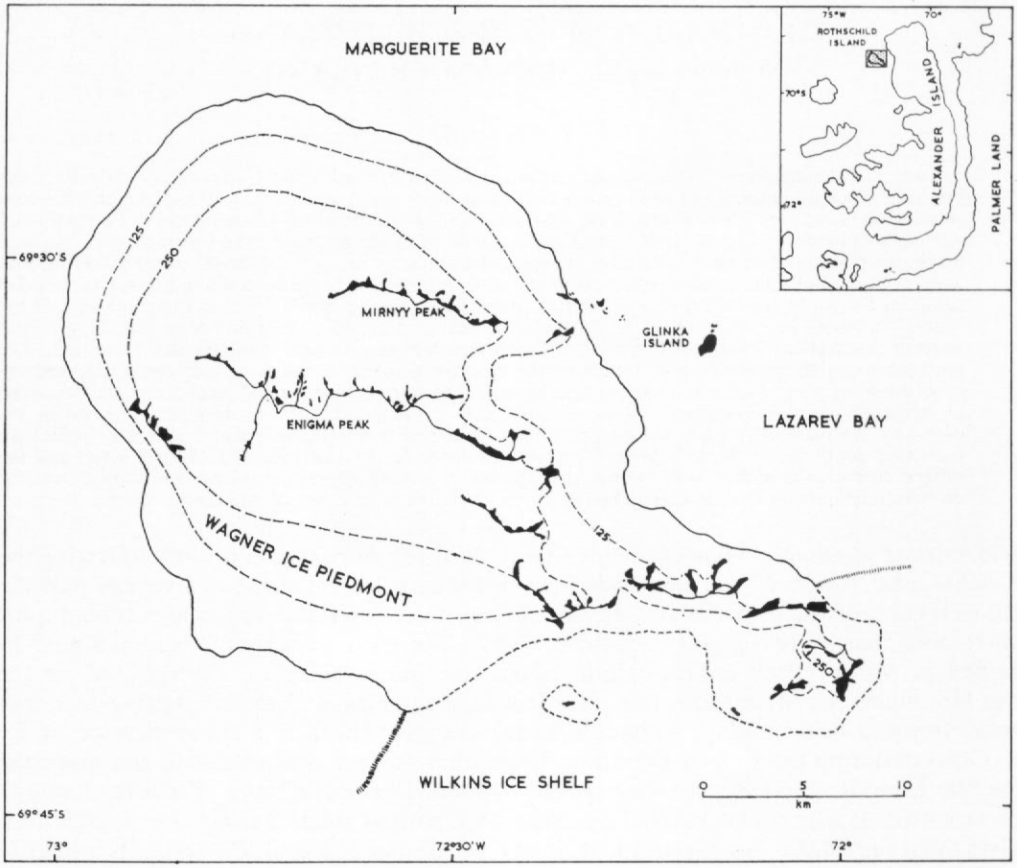

Fig. 1. Topographical sketch map of Rothschild Island. The positions of rock outcrops are marked in black. The inset shows the position of Rothschild Island in relation to the Antarctic Peninsula.

from the lower Wagner Ice Piedmont in the south and its mountainous extension in the south-east (Fig. 1). This range also divides the island into two areas of contrasting topography related to the weathering of different rock types (Fig. 2 a and b): well-jointed granitic rock on the ridges in the north of the island forms short steep-sided buttresses and north-facing walls, while in the south-east the often steeply dipping sedimentary rocks have produced jagged ridges and peaks (Fig. 3) with south- and south-west-facing cliffs. Along the east coast in Lazarev Bay, marine erosion of the sediments has formed small rocky islands, headlands and sea stacks (Fig. 4) and, in the south-east, weathering of relatively unconsolidated volcanic rock has resulted in rounded, predominantly scree-covered outcrops. Erosion along probable west-north-west to east-south-east trending faults has determined the general parallel alignment of mountain ranges and rock ridges on the island.

General Stratigraphy

The sequence of geological events on Rothschild Island is shown in Table I together with the corresponding events in Alexander Island. The oldest rocks are folded and locally sheared mudstones, sandstones and conglomerates similar to rocks found in northern, central and southern Alexander Island.

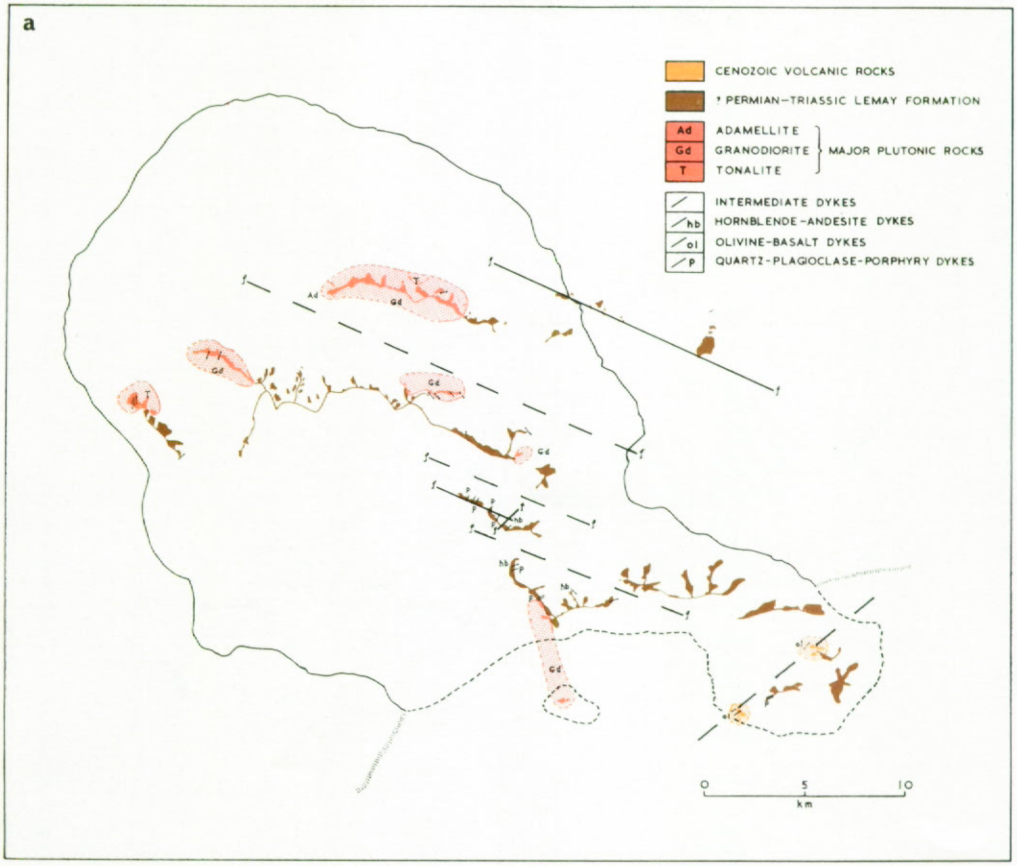

Fig. 2. a. Geological sketch map of Rothschild Island.

Edwards (in press) has proposed the overall name LeMay Formation for these rocks and has determined a Middle–Upper Triassic age for a varied invertebrate faunal assemblage from part of the sequence cropping out in the Lully Foothills of central Alexander Island.

These sediments were subjected to varying degrees of folding and cataclastic deformation during the "Gondwanian" orogeny of late Triassic–early Jurassic times (Dalziel and Elliot, 1973), prior to the intrusion of hornblende-andesite dykes. Similar dykes from northern Alexander Island (Bell, 1974) are thought to be feeders for the tuffs, lavas and agglomerates of the Elgar Uplands volcanic sequence, which has an apparent K-Ar age of 70 Ma in the Colbert Mountains (Grikurov and others, 1967) and an inferred early Cenozoic age in the Elgar Uplands (Thomson and Burn, 1977). No volcanic rocks belonging to this sequence occur on Rothschild Island.

Six plutons, having a predominantly granodioritic composition but varying from adamellite to tonalite, were then emplaced into the sediments of the LeMay Formation. They are comparable to granodioritic rocks from the Rouen Mountains batholith of northern Alexander Island which have a probable Tertiary age (Care, in press). Thin near-vertical acid and intermediate dykes cut both the plutonic and sedimentary rocks.

Two isolated outcrops of bedded palagonite-tuff and lapillistone intruded by olivine-basalt dykes occur in south-eastern Rothschild Island. These closely resemble volcanic rocks found

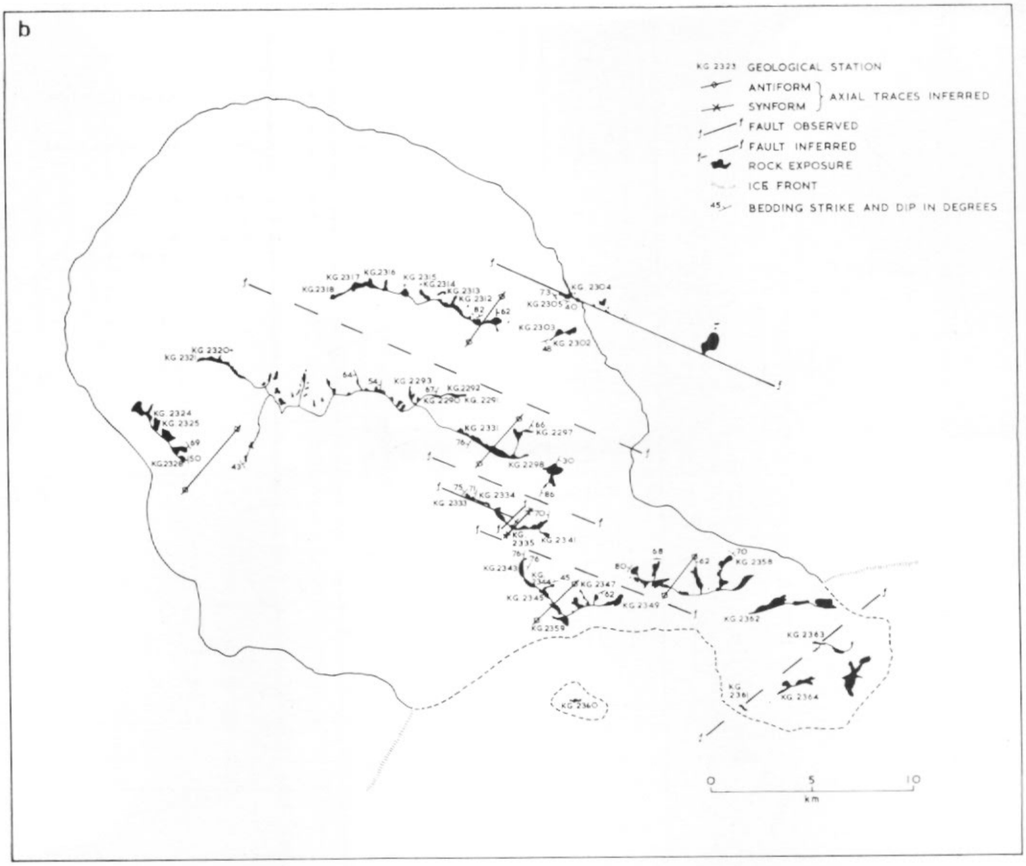

Fig. 2. b. Structural sketch map of Rothschild Island showing the positions of geological stations.

in Beethoven Peninsula of south-western Alexander Island (Bell, 1973) and in the Elgar Uplands of northern Alexander Island (personal communication from R. W. Burn), and form part of a wide belt of Cenozoic volcanic rocks extending through western Antarctica and having ages from Oligocene (26–29 Ma) to Quaternary (0.2 Ma) (LeMasurier and Rex, in press).

LeMay Formation

Folded and locally sheared unfossiliferous sediments, similar to the (?) Permian–Triassic LeMay Formation sediments exposed in northern Alexander Island (Care, 1977; personal communication from R. W. Burn), are widely distributed on Rothschild Island and comprise purple-grey and grey-green sandstone, mudstones, pebble-conglomerates and mud-flake breccias. The arenaceous rocks are immature both texturally and mineralogically and, because of their high content of silty matrix (30–55%; Table II), they are classified as feldspathic and lithic greywackes (Pettijohn and others, 1972). These sediments are generally massively bedded and depositional features are restricted to small-scale load structures, graded bedding in the rudaceous rocks, and rare small-scale cross bedding. At station KG.2304, a 60 cm thick conglomerate bed shows an upward decrease in size and an increase in abundance of clasts, with pebbles up to 2 cm across at the base to granules <4 mm at the top which possess an

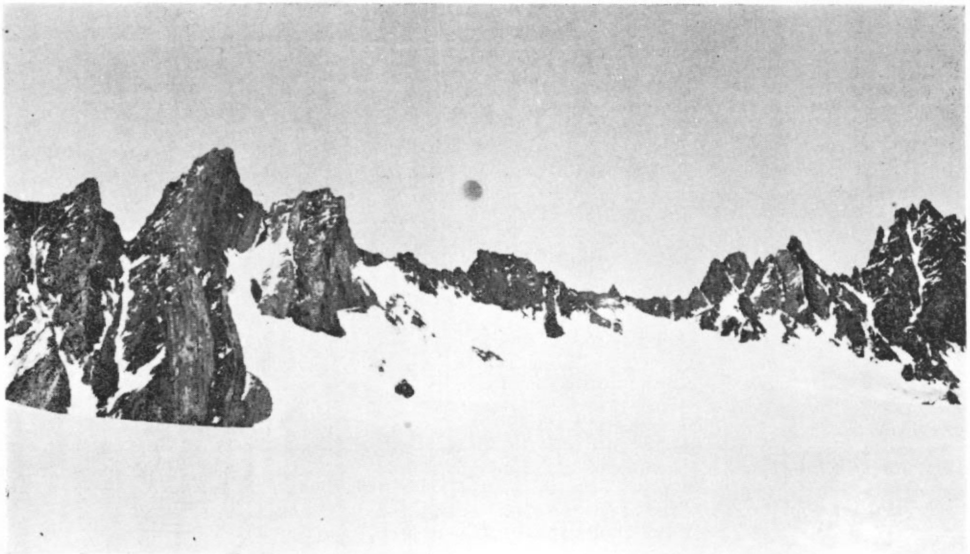

Fig. 3. Steeply dipping beds of the LeMay Formation forming a jagged ridge in the south of Rothschild Island. A dyke has been intruded along a folded bedding plane in the windscoop on the left. The relief is approximately 120 m.

Fig. 4. The rocky islands in ice-filled Lazarev Bay (Glinka Island in the distance) off the north-easternmost headland of Rothschild Island, formed by marine erosion of deformed LeMay Formation sediments. A high-angle fault, cutting the 20 m cliff in the foreground, can be traced across the bay to truncate the southern ends of the islands.

TABLE I. SEQUENCE OF GEOLOGICAL EVENTS IN ROTHSCHILD ISLAND AND THE EQUIVALENT FORMATIONS IN ALEXANDER ISLAND

	Rothschild Island	*Alexander Island*
Cenozoic	Olivine-basalt dykes Palagonite-tuffs and lapillistones	Beethoven Peninsula volcanic sequence
(?) Tertiary	Intermediate dykes	
	Quartz-plagioclase-porphyry dykes Aplite and pegmatite intrusions Adamellite Granodiorite Tonalite	Rouen Mountains batholith
L. Tertiary–U. Cretaceous	Hornblende-andesite dykes	Elgar Uplands volcanic sequence
(?) Permian–Triassic	Mudstones, greywackes and conglomerates (locally sheared)	LeMay Formation

imbricate structure parallel to the bedding. An erosional contact exists between the base of this bed and the underlying laminated sandstone.

Tectonically deformed sediments are seen at only a few localities and these take the form of sheared conglomerates in which the clasts have been flattened and aligned sub-parallel within a highly sheared matrix. A thin section of the matrix from specimen KG.2331.1 displays oval-shaped clasts of a poorly sorted sandstone, containing quartz, feldspar, biotite and rare volcanic and sedimentary fragments set in a brown flow-orientated matrix of microcrystalline quartz, feldspar and sericite. Sheared, rubbly weathering interbedded sandstone and mudstone up to 20 cm thick, with some boudinaging of the more competent layers, form a series of rocky spires and nunataks in the north-east of the island (KG.2302 and 2303). Similar dark-coloured rock forms Glinka Island and the islets to the east in Lazarev Bay.

A 15 cm wide clastic dyke cuts greywacke and pebble-conglomerate beds in a small exposure at station KG.2304. Petrographical examination (KG.2304.3) shows the rock is a feldspathic greywacke containing a much higher percentage (21 %) of feldspar fragments compared to the other sections examined (2.2–13.3 %) and a more varied heavy mineral assemblage. Numerous clastic dykes have been described from the Mesozoic succession of south-eastern Alexander Island (Taylor, 1966) and some of these have been formed by the upward injection of material from a lower stratigraphical level, possibly as the result of the weight of overburden coupled with fissuring caused by seismic disturbances in an unstable shelf environment. The only occurrences of similar dykes in the older sediments of the Antarctic Peninsula have been recorded by Hooper (*in* Taylor, 1966) from the "Trinity Peninsula Series" at Hope Bay, north-eastern Graham Land, and by R. W. Burn (personal communication), who found several small clastic dykelets in the LeMay Formation. It could not be determined, because of the nature of the exposure, whether the dyke on Rothschild Island had originated by upward injection of material or by gravity infilling of a fracture. Networks of small veins up to a few millimetres across, composed of silt with angular quartz grains up to 0.05 mm, are common throughout the arenaceous sediments and are also seen within the sedimentary clasts from the pebble-conglomerates.

In the field, the sediments occur as two types with distinctly different colours: those possessing a deep purple-grey colour in which rust-weathering was common; and those with a grey-

TABLE II. MODAL ANALYSES OF SEDIMENTS FROM THE LEMAY FORMATION ON ROTHSCHILD ISLAND

	1	2	3	4	5	6	7
Quartz	36.6	19.2	23.6	17.6	15.1	36.0	29.3
Plagioclase	8.8	19.6	7.8	11.9	3.8	11.2	6.1
K-feldspar	2.4	1.4	1.8	1.6	0.4	2.1	1.6
Volcanic fragments	4.0	7.5	13.2	9.1	12.6		5.4
Sedimentary fragments	7.3	1.3	15.7	1.3	30.5	7.9	10.0
Metamorphic fragments	1.2	3.1	5.0	1.9	2.3		0.7
Plutonic fragments	0.7	0.8	1.1	0.5	4.3		3.4
Biotite	0.8	0.2	0.4	tr	0.4	3.4	1.1
Muscovite	0.2	tr	tr	—	tr	—	—
Chlorite	tr	0.4	tr	—	0.8	—	—
Hornblende	—	1.4	—	—	—	—	—
Augite	0.1	0.2	—	—	—	—	—
Sphene	0.2	0.1	tr	0.1	—	tr	—
Opaques	0.2	0.2	0.3	0.1	0.4	0.3	0.4
Zeolite	tr	0.5	tr	0.5	—	tr	—
Zircon	tr	tr	—	tr	tr	tr	tr
Matrix	37.5	44.1	31.1	55.4	29.4	39.1	42.0
Quartz	60.0	36.3	34.6	40.1	9.6	63.0	51.9
Feldspar	18.4	39.7	14.0	30.8	2.6	23.2	13.6
Rock fragments	21.6	24.0	51.4	29.1	87.8	13.8	34.5
Plutonic and metamorphic	14.4	30.7	17.4	18.8	13.3	—	21.0
Volcanic	30.3	59.1	37.7	71.0	25.3	—	27.7
Sedimentary	55.3	10.2	44.9	10.2	61.4	—	51.3

tr Trace.

1. KG.2297.4 Lithic greywacke; central Rothschild Island.
2. KG.2304.3 Sedimentary dyke; north-east Rothschild Island.
3. KG.2341.1 Mud-flake breccia; central Rothschild Island.
4. KG.2343.2 Feldspathic greywacke; southern Rothschild Island.
5. KG.2344.1 Matrix of pebble-conglomerate; southern Rothschild Island.
6. KG.2349.1 Lithic greywacke; southern Rothschild Island.
7. KG.2362.1 Mud-flake breccia; south-east Rothschild Island.

green hue and little if any surface staining. The deep purple variants include mudstones, banded sandstones and finer-grained sediments up to mud-flake breccias, whereas the grey-green rocks have a wider textural range from medium and coarse sand grade to mud-flake breccias and pebble-conglomerates. Both colour variants have an irregular distribution throughout the island and are interbedded in many outcrops.

Petrographical examination shows the purple and green colours are due to the presence of very fine-grained biotite and chlorite, respectively, in the matrix of the sediments, as distinct from the larger detrital flakes of the same minerals. Much of the chlorite is authigenic but the biotite is probably detrital and not of metamorphic origin, because it occurs in sediments unrelated to the known plutonic intrusions on the island with virtually no recrystallization of the groundmass, and detrital zeolites are often present. Similar fine-grained biotite scattered throughout some of the volcanic and sedimentary clasts indicates a possible source for the mineral.

Pebble-conglomerates

Horizons of conglomerate are uncommon and generally occur as units less than 1 m thick interbedded with greywackes but, in a massive exposure of well-jointed conglomerate forming a 25 m long ridge (KG.2344), the true thickness of the bed is unknown as bedding features are absent. In the hand specimen, the rudaceous rocks are polymict, containing rounded and sub-angular pebbles of plutonic, volcanic, sedimentary and metamorphic material (Fig. 5), commonly in the size range 1–6 cm, with occasional cobbles up to 20 cm. Grey mudstone, pale yellow and green sandstone, and laminated sandstone, quartzite, quartz-mica-gneiss, granite and trachytic and porphyritic lava fragments are enclosed in a coarse grey-green greywacke matrix. The sedimentary clasts are the most abundant and have the largest dimensions, whereas the other lithic material rarely exceeds 4 cm in diameter.

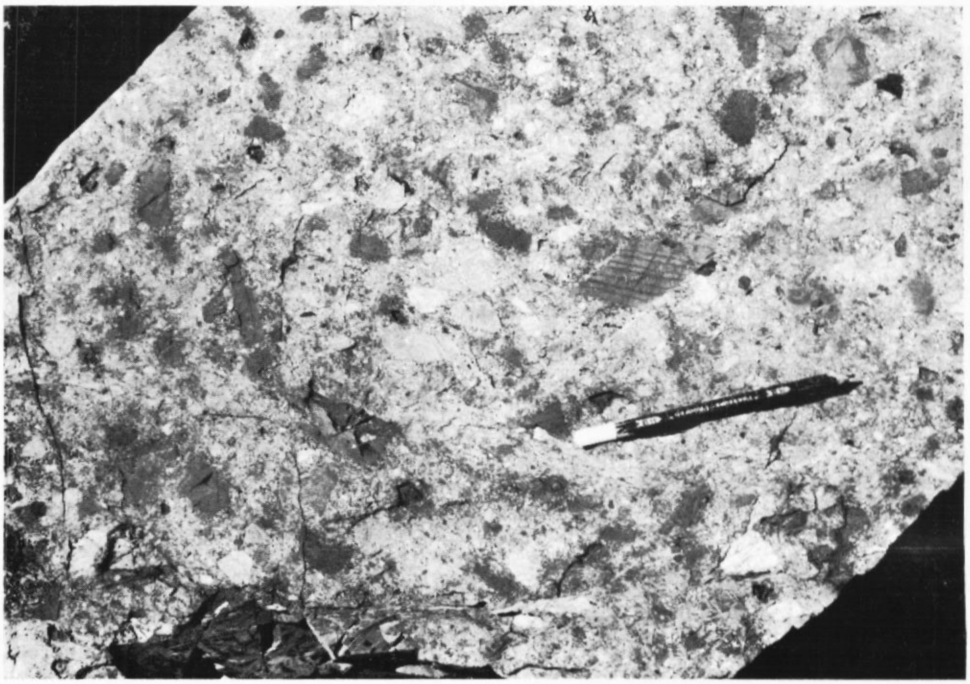

Fig. 5. Joint surface of a conglomerate displaying sub-angular pebbles of mudstone and quartzite. The pencil is 13 cm long.

Mud-flake breccias

Small oval-shaped mudstone pellets and flakes up to 2 mm long are present within nearly all of the arenaceous sediments but larger angular clasts are concentrated in beds of mud-flake breccia up to 20 cm thick (KG.2358) which often show grading of the clasts and contacts with adjacent beds displaced by minor faulting (Fig. 6). These intraformational breccias comprise tabular slabs of dark grey mudstone in a sandy matrix and owe their elongated nature to their brecciated origin. The frequent parallel alignment of clasts is a primary sedimentary feature and not the result of tectonic deformation.

Greywackes

Feldspathic and lithic greywackes are the most abundant of the sediments and form exposures of massive, ungraded dark green and purple rock. They are mostly of medium to coarse sand grade and contain conspicuous grains of pink feldspar, vitreous quartz, black mica and golden iron ore, up to 1 mm across, in addition to a variable content of dark grey mudstone clasts, all within a dirty brown-green chloritic and quartzo-feldspathic cement. The finer-grained rocks commonly display small-scale colour bands ($\leqslant$1 cm thick) and in specimen KG.2349.1 the darker layers are seen to contain microscopic concentrations of biotite and iron ore.

Mudstones

Argillaceous rocks are rare. They occur as dark grey to black mudstone horizons (up to 20 cm thick) and thin laminae (down to 2 mm in thickness) frequently interbedded with arenaceous material.

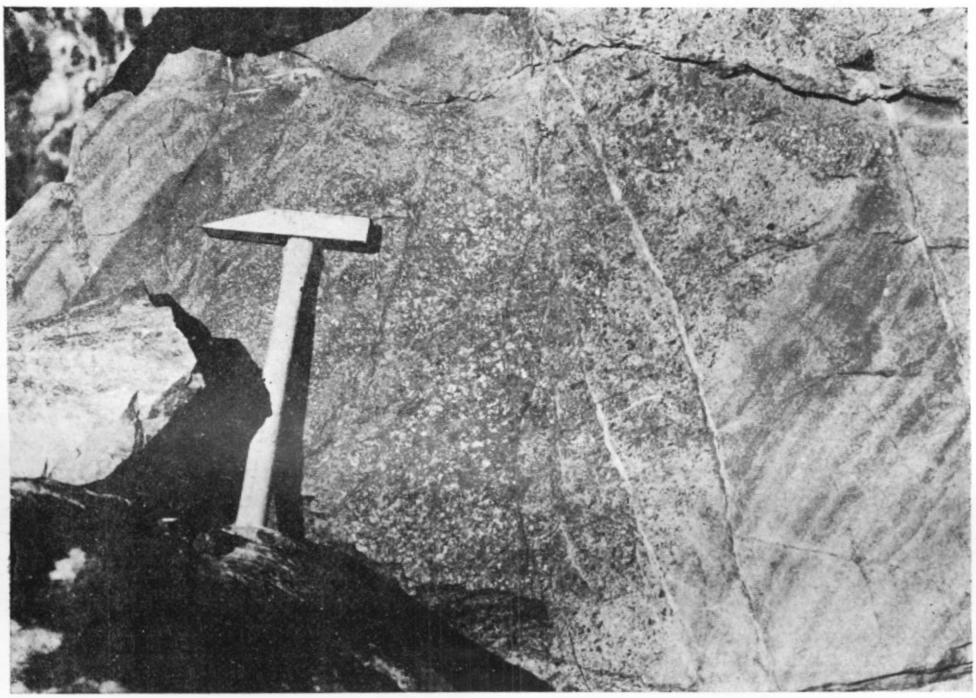

Fig. 6. A graded mud-flake breccia horizon from the LeMay Formation of south-east Rothschild Island displaying a faulted lower contact with colour-banded sandstone. The hammer shaft is 35 cm long.

Mineralogy

Modal analyses of six greywackes and mud-flake breccias, and the matrix of a pebble-conglomerate are given in Table II.

Quartz is present in all the sedimentary rocks as unstrained angular fragments and rounded grains up to 1.6 mm in length (KG.2362.1). Occasional embayed quartz grains are present, suggesting a volcanic source of material, and polycrystalline aggregates of strained quartz indicate either a plutonic or metamorphic origin.

Plagioclase of a predominantly andesine composition forms the major part of the total feldspar content of the sediments, while potash feldspar is represented by perthite with smaller amounts of microcline. All the feldspars are angular and of similar size to the quartz grains and the twin lamellae of the andesines are frequently bent and broken. Alteration to sericite and calcite is present but is not widespread.

Rock fragments form a considerable proportion of the allogenic material in the sediments and 50% of the conglomerate matrix (KG.2344.1) is composed of sand-sized lithic fragments. The proportions of the different types of lithic fragments are shown in Fig. 7, indicating a predominantly sedimentary and volcanic source for the material. Indigenous material includes flakes and pellets of dark brown-green mudstone with some fine-grained greywacke and rare sheared sandstone clasts (KG.2341.1). The exotic fragments comprise mostly fine-grained lavas with a pilotaxitic texture of feldspar microlites enclosing a peppering of opaque material and rare phenocrysts of sericitized plagioclase. These clasts reach 3 mm in size in specimen KG.2297.4. Plutonic rock fragments (up to 1.6 mm in specimen KG.2341.1) are represented by granitic and granodioritic clasts comprising bonded grains of quartz, plagioclase or perthite;

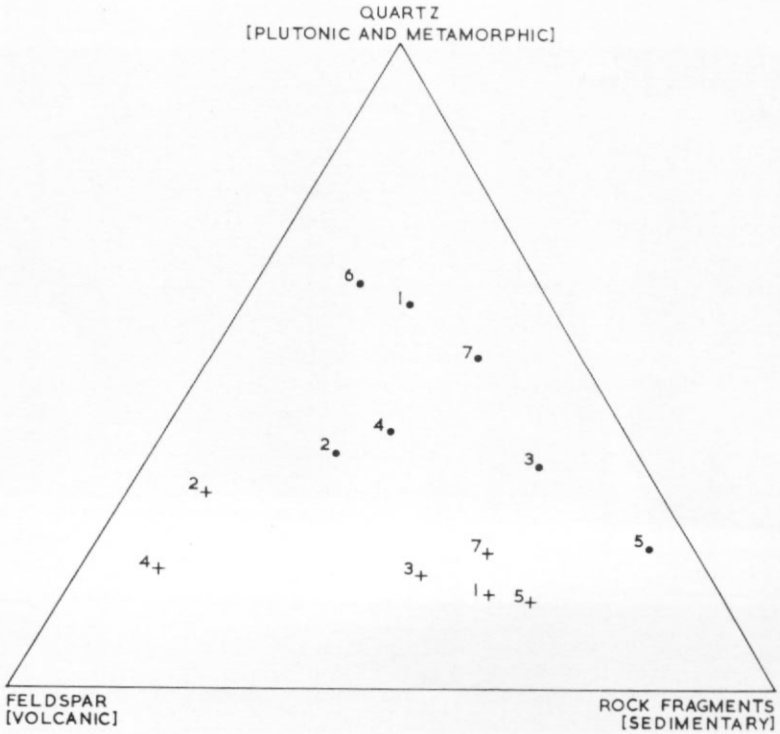

Fig. 7. Ternary diagram showing the composition of the LeMay Formation sedimentary rocks (●) and their component lithic fragments (+).

TABLE III. MODAL ANALYSES OF PLUTONIC ROCKS FROM ROTHSCHILD ISLAND

	1	2	3	4	5	6	7	8	9	10	11	12	13	14	15	16	17	18
Quartz	21.8	30.7	20.3	39.8	36.8	20.4	31.5	32.4	39.4	20.9	19.2	11.3	0.6	1.5	26.2	26.8	0.1	18.3
Alkali-feldspar	12.2	8.3	11.5	19.8	14.3	4.7	14.5	15.3	22.3	15.0	3.6	—	—	—	11.2	12.0	—	2.5
Plagioclase	46.4	44.7	49.2	33.4	37.5	47.1	41.5	37.5	30.7	44.4	50.5	29.9	12.5	12.6	40.1	40.7	1.1	59.3
Olivine	—	—	—	—	—	—	—	—	—	—	—	—	—	—	—	—	10.6	—
Clinopyroxene	—	—	1.0	—	—	0.8	—	—	—	tr	—	—	—	3.9	—	—	7.5	—
Orthopyroxene	tr	—	tr	—	—	—	—	—	—	—	—	—	—	—	—	—	2.3	—
Hornblende	10.3*	10.6*	10.8	—	5.0	13.0	5.8	7.2*	1.7*	15.5*	15.8*	—	7.7*	7.1	13.2*	13.8	—	11.5†
Biotite	7.1	4.4*	6.4*	6.2*	5.6*	[illegible]	6.1*	[illegible]	5.2*	2.8*	10.2*	1.6*	—	—	8.0*	4.5*	—	8.1†
Chlorite	—	—	—	—	—	—	—	—	—	—	—	—	1.2	—	—	—	—	—
Iron ore	2.2	1.3	0.8	0.8	0.8	2.7	0.6	0.9	0.7	1.4	0.7	0.2	—	0.2	1.3	2.2	—	0.3
Other minerals	tr	tr	—	tr	—	tr	—	tr	—	tr	tr	—	tr	tr	tr	tr	tr	—
Groundmass	—	—	—	—	—	—	—	—	—	—	—	57.0	78.0	74.7	—	—	78.4	—
Vesicles	—	—	—	—	—	—	—	—	—	—	—	—	—	—	—	—	21.4‡	—
Plagioclase composition	An_{27-51}	An_{26-34}	An_{31-53}	An_{30-43}	An_{27-47}	An_{23-54}	An_{28-63}	An_{24-48}	An_{30-48}	An_{30-57}	An_{33-57}	An_{24-34}	An_{29-53}	An_{28-58}	An_{26-48}	An_{28-53}	An_{48-63}	An_{37-48}

tr Trace.
* Includes alteration to chlorite.
† Mostly altered to iron ore.
‡ Vesicle proportion is discounted in the mineral percentages but shown as percentage of total rock.
(Minimum of 1 000 points counted per section.)

1. KG.2291.6 Granodiorite; central Rothschild Island (average of two analyses).
2. KG.2292.1 Granodiorite; central Rothschild Island.
3. KG.2293.1 Granodiorite; central Rothschild Island (average of two analyses).
4. KG.2298.1 Granodiorite; central Rothschild Island (average of two analyses).
5. KG.2312.5 Granodiorite; northern Rothschild Island.
6. KG.2314.1 Tonalite; northern Rothschild Island.
7. KG.2316.1 Granodiorite; northern Rothschild Island.
8. KG.2317.4 Granodiorite; northern Rothschild Island.
9. KG.2318.1 Adamellite; northern Rothschild Island.
10. KG.2321.4 Granodiorite; western Rothschild Island (average of two analyses).
11. KG.2324.1 Tonalite; western Rothschild Island (average of two analyses).
12. KG.2333.1 Quartz-plagioclase-porphyry dyke; central Rothschild Island.
13. KG.2343.7 Hornblende-andesite dyke; southern Rothschild Island.
14. KG.2347.1 Hornblende-andesite dyke; southern Rothschild Island.
15. KG.2359.8 Granodiorite; southern Rothschild Island.
16. KG.2360.1 Granodiorite; southern Rothschild Island.
17. KG.2363.2 Hypocrystalline olivine-basalt dyke; south-eastern Rothschild Island.
18. KG.2363.3 Tonalite xenolith from olivine-basalt dyke; south-eastern Rothschild Island.

[face page 97

several grains of myrmekite are present. The metamorphic clasts (0.8 mm long in specimen KG.2297.4) are polycrystalline aggregates of quartz with occasional plagioclase and rare flakes of muscovite (quartz-muscovite-gneiss).

Detrital ferromagnesian minerals form only a small part of the allogenic material in the sediments. The chief mineral is biotite, occurring as bent and broken subhedral plates up to 0.9 mm (KG.2304.3), often impinged on quartz and feldspar grains. Anhedral augite and hornblende, as fractured grains, occur in the sedimentary dyke (KG.2304.3) where they reach 0.6 mm. In some thin sections, fine-grained aggregates of anhedral biotite occur in the matrix, giving the rock a characteristic purple colour in the hand specimen. Other detrital minerals include magnetite, haematite, zircon, sphene, muscovite (forming contorted plates up to 0.8 mm impinged on quartz grains in specimen KG.2304.3) and chlorite. The last reaches 0.2 mm as individual flakes but it is commoner as a felt-like cement in some rocks, giving them a greenish tinge. Zeolites (? thomsonite) are seen in several of the rocks examined and they appear to be detrital fragments of lavas rather than of authigenic origin.

Contact Metamorphic Rocks

Contact metamorphic aureoles containing rocks up to the albite-epidote-hornfels grade surround most of the plutons on the island. The LeMay Formation sediments within 0.5 km of intrusive contacts are hornfelsed, with bleaching and recrystallization of arenaceous rocks and the growth of spots in argillaceous material.

A feldspathic greywacke in contact with the tonalite at station KG.2325 displays a granoblastic polygonal texture with relict grains of fractured and strained quartz, orthoclase and andesine up to 0.9 mm and abundant biotite porphyroblasts in a recrystallized mosaic (average size 0.1 mm) of quartz with chlorite, sericite, muscovite, iron ore, sphene and zircon. At station KG.2290, in the contact zone with a granodiorite, the LeMay Formation sediments have been altered to a pale yellow-grey colour and recrystallized to a fine aggregate of quartz and feldspar. They are cut by several thin (1–3 cm) black pneumatolytic veins which weather to a pumice-like surface. These veins comprise abundant tourmaline (? schorlite) as laths up to 0.8 mm long with transverse fractures and smaller anhedral crystals with zoned triangular basal sections, together with haematite, fluorite, anhedral topaz and calcite.

Adjacent to the granodiorite intrusion in the south of the island (KG.2345), the fine-grained sediments have been thermally metamorphosed to dark-coloured hornfelses comprising microcrystalline quartz and feldspar with vague round and oval-shaped spots from 0.3 to 0.6 mm in diameter. The nuclei of these spots appear to be formed of sphene and pale green pleochroic epidote, and are surrounded by a border of sericite-rich material which interconnects the spots. In some cases, growth of epidote has pushed the sphene granules to the margins of the spots. Small iron-ore cubes and anhedral crystals are scattered throughout the thin section and appear unrelated to the growth of the spots.

Major Intrusive Rocks

Six small plutons from 25 km^2 to less than 2 km^2 in area (Fig. 2a) intrude folded sediments of the LeMay Formation on Rothschild Island. These plutons have an irregular distribution, most occurring in the north of the island, and they probably represent the cupolas of a large intrusion at depth. They have distinctive mineralogies (Table III) and their compositions range from tonalite to adamellite but granodiorite predominates (Fig. 8). All the plutons are xenolithic with rounded inclusions of both sedimentary and igneous material from the common 2 cm to 15 cm by 15 cm across at station KG.2321. The rocks form well-jointed exposures and typically possess a coarse to medium hypidiomorphic granular texture.

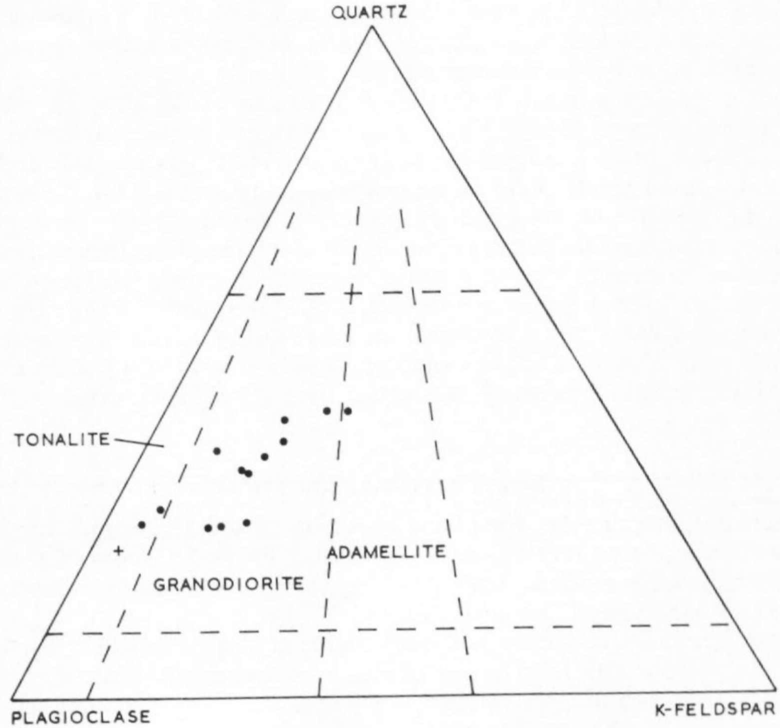

Fig. 8. Ternary diagram showing the modal composition of major intrusive rocks (●) and a tonalite xenolith (+) from Rothschild Island (after Nockolds, 1954).

Intrusive contacts with the LeMay Formation are generally sharp but on the ridge exposure at station KG.2290 the contact is marked by a 10 m zone of country rock criss-crossed by irregular, porphyritic granodioritic apophyses up to 1 m in width. Mineralization, in the form of abundant euhedral cubes of pyrite (up to 2 mm), is seen in this zone and elsewhere pyrite disseminations are common within the granodiorites, with malachite coatings on some joint planes and malleable silvery plates of molybdenite up to 5 mm across within a pegmatite vein at station KG.2315.

Intermediate dykes were only seen to intrude the four northernmost plutons on the island, and aplite and pegmatite veins are of minor importance.

Tonalite

Tonalite crops out north of Mirnyy Peak (KG.2314), where it occurs as a marginal variety to the granodiorite, and in a separate intrusion cutting the northern part of the ridge to the west of Enigma Peak (KG.2324). Quartz and orthoclase with rare perthites form poikilitic plates up to 3 mm across and are interstitial to zoned plagioclase (An_{23-57}) laths, which comprise approximately 50% of the rock, and a considerable amount of mafic minerals with hornblende slightly more abundant than biotite. Both hornblende (α = yellow-green, β = olive-green, γ= dark green and $\gamma : c = 12$–$17°$) and biotite (α = straw, $\beta = \gamma$ = deep green-brown) occur as subhedral crystals up to 3 mm across and in aggregates up to 7 mm across with partial alteration to chlorite and iron ore, and inclusions of apatite and sphene. Some hornblende forms a secondary alteration rim around colourless augite ($\gamma : c = 54°$) (KG.2314.1). Accessory minerals include epidote, iron ore and allanite.

Granodiorite

Granodiorite is the major component of the plutons on the island with the exception of the tonalite exposure in the extreme west. Clear, fractured anhedral quartz forms phenocrysts up to 8 mm across in specimen KG.2298.1 with smaller anhedral crystals of quartz and cloudy brown orthoclase in the groundmass. Perthites are rare but the development of a graphic texture occurs in the pluton to the east of Enigma Peak (KG.2291–93). Plagioclase (oligoclase-labradorite) commonly forms subhedral laths up to 4.5 mm in length with zoning and variable sericitization. Hornblende (α = pale yellow-green, β = mid green, γ = deep green and $\gamma : c = 14$–$19°$) and biotite (α = straw, $\beta = \gamma$ = deep red-brown) are found as euhedral to subhedral crystals and aggregates of anhedral crystals in varying proportions throughout the plutons, and all show partial alteration to chlorite. Biotite is the only mafic mineral present in specimen KG.2298.1 and is of equal importance to hornblende within the granodiorite of the Mirnyy Peak range. Elsewhere, hornblende is the dominant mafic mineral and forms euhedral phenocrysts which reach 1 cm in length in specimen KG.2360.1. The hornblende crystals occasionally display a sieve texture with inclusions of quartz and opaque ores. Augite, as small, colourless fractured crystals, is seen in a few of the granodiorites but it is invariably altered to hornblende and fibrous tremolite. Accessories include sphene, iron ore, epidote and usually apatite.

Adamellite

A single outcrop of adamellite occurs at the western end of the ridge including Mirnyy Peak and differs from the other plutonic rocks in having a higher percentage of potash feldspar, consisting almost entirely of braid and flame perthite, and a lower mafic mineral content (Table III).

Minor Intrusive Rocks

Dykes are widespread throughout the island. They include the conspicuous hornblende-andesite and quartz-plagioclase-porphyry dykes encountered exclusively within the LeMay Formation of southern Rothschild Island, and a swarm of porphyritic and aphyric dykes of intermediate composition, which cut both the sediments and the granodioritic intrusions. The majority of the dykes are vertical or near-vertical which can be attributed to intrusion along steeply inclined bedding planes within the LeMay Formation (Fig. 3) or along vertical joints within the granodiorite.

Field evidence indicates that the intermediate dykes are the youngest of the minor intrusive rocks as they intrude a hornblende-andesite dyke at station KG.2343, a pegmatite sill at station KG.2313 and the granodiorites at several localities. The hornblende-porphyry intrusions are presumably older than the major plutonic episode as they do not cut the plutons and rounded porphyritic xenoliths of a similar composition often appear within the granodiorites.

No age relationships could be determined for the quartz-plagioclase-porphyry dykes, despite the fact that all those observed occur within a few metres of both intermediate and hornblende-andesite intrusions, but they are inferred to be late products of the major plutonic episode.

Hornblende-andesite dykes

These sharply defined dykes vary from 2.5 to 10 m in width, have pale grey-green weathering patinas and display conspicuous euhedral hornblende phenocrysts up to 2 cm in length accompanied by smaller (1 cm) crystals of plagioclase, pyroxene and quartz. The fine- to medium-grained, dark grey-green matrix is dominated by feldspar laths with variable amounts of hornblende, augite and iron ore.

Subhedral plagioclase phenocrysts (oligoclase-labradorite) are mostly sericitized or have their fractures infilled by calcite (KG.2343.7); the composition of the groundmass feldspar could not be determined. Quartz occurs as small grains and rarely as embayed xenocrysts up to 2.5 mm with reaction rims of small augite crystals or a mat of calcite and epidote crystals. Subhedral augite ($\gamma : c = 46–50°$) up to 0.4 mm is common throughout the matrix of specimen KG.2347.1, often forming glomeroporphyritic clusters; in specimen KG.2343.7 it is pseudomorphed by interlocking aggregates of penninite and calcite. Hornblende (α = pale green, β = green, γ = dark green and $\gamma : c = 14–17°$) is frequently twinned and poikilitic to quartz, feldspar and iron ore. The accessory minerals include apatite, chlorite, epidote and iron ore, and (?) thomsonite is a common interstitial mineral in specimen KG.2343.7.

Late intermediate dykes

The most abundant of the minor intrusions are dykes of andesitic composition, usually 1–4 m wide, with sharp contacts against the country rock and reddish alteration staining on exposed surfaces. Quartz, feldspar, epidote and occasionally hornblende are visible in the hand specimen as phenocrysts up to 5 mm in length within a fine-grained, mid pale green groundmass; aphyric andesite dykes are rare.

In thin section, the dykes show considerable hydrothermal alteration. Quartz is a rare interstitial mineral but in the hornblende-andesite (KG.2364.2) it is present as numerous corroded xenocrysts up to 3 mm across with alteration rims of very fine-grained biotite. Plagioclase (andesine-labradorite) is mostly altered to epidote and calcite, and in specimen KG.2364.2 albitization is widespread. Ragged sieved plates and rare euhedral zoned crystals (KG.2328.3) of hornblende (α = pale yellow, β = yellow-green, γ = brown-green and $\gamma : c = 15–17°$) are common throughout the groundmass of many of the dykes. Pyroxenes were only seen in the two dykes cutting the granodiorite intrusion to the west of Enigma Peak; subhedral to anhedral augite ($\gamma : c = 46–53°$) up to 1 mm with simple and multiple twinning is seen in specimen KG.2302.2, whereas hypersthene, partially altered to chlorite, forms rare subhedral laths in specimen KG.2321.9. Antigorite, prochlorite and penninite pseudomorphs after hornblende and pyroxene are common and accessory minerals include magnetite (as individual crystals up to 0.4 mm in specimen KG.2335.3), haematite, epidote and sphene. The groundmass is composed essentially of microcrystalline plagioclase with smaller amounts of quartz and mafic minerals which, in specimen KG.2321.9, impart a trachytic texture to the rock.

Quartz-plagioclase-porphyry dykes

Pale cream-coloured porphyry rock forms dykes from 3 to 15 m in width and with general north–south trends, which are often highly shattered by weathering action and contain little *in situ* rock. Rounded subhedral phenocrysts of clear quartz and orange-yellow weathered feldspar up to 1 cm across occur within a microcrystalline, pale grey-green groundmass of quartz, feldspar and sericite.

Chlorite pseudomorphs after biotite are common and are invariably streaked with opaque minerals. The fractured quartz crystals have deeply embayed faces but are generally free from inclusions, unlike the plagioclase which is poikilitic to quartz, chlorite and groundmass material. Phenocrysts are often rimmed by radiating growths of feldspar which also form discrete spherules up to 1.5 mm in diameter within the groundmass. The altered plagioclase (oligoclase-andesine) contains much epidote and calcite; magnetite and haematite are rare accessory minerals (Table III).

Aplites and pegmatites

Dykes, sills and veins of aplite and pegmatite are sharply defined but of limited occurrence with the aplite dykes varying in size from 35 cm at station KG.2360 to 3 cm at station KG.2312 and the rarer pegmatite intrusions ranging from 15 cm to less than 1 cm. The pegmatites possess medium-grained saccharoidal margins of quartz and potash feldspar enclosing cores of coarse quartz crystals (many exhibiting bipyramidal forms) and pink feldspars with scattered concentrations of epidote and (?) hornblende. The aplites are the medium- to fine-grained equivalents of the pegmatites and they have an overall pink to grey colour.

Geochemistry

Ten analyses of plutonic and hypabyssal rocks from Rothschild Island are given in Table IV; six of the specimens are from the major plutons (five granodiorites and one tonalite); one is a specimen from a quartz-plagioclase-porphyry dyke; one specimen is from the intermediate dyke suite; and the final two are specimens of the pre-plutonic hornblende-andesite dykes. Values for MnO are not yet available but they are expected to be low, between 0.14 and 0.08% (Le Maitre, 1976).

The analyses of the major plutonic rocks show a gradual increase in the contents of alkali metals (sodium and potassium) and calcium when plotted on A–F–M and Ca–Na–K diagrams, respectively (Fig. 9). These trends are indicative of calc-alkaline rock suites (e.g. Mount Lassen; Nockolds and Allen, 1953) and are persistently richer in magnesium and poorer in sodium than the corresponding trends for Graham Land plutonic rocks as determined by Adie (1955). The trends, however, are similar to those obtained for other areas of the Antarctic Peninsula (West, 1974; Davies, 1976; Singleton, 1976; Smith, 1977), where the differences from the earlier trends obtained by Adie (1955) have been partially attributed to the different analytical techniques employed.

The four hypabyssal rocks also fall on the general trend of alkali enrichment (Fig. 9), possibly indicating derivation and differentiation from the same or a similar parental magma. Further genetic relationships are implied when certain inter-element ratios are compared (Table V) for the plutonic and hypabyssal rocks. The major plutonic rocks show a gradual increase in Zr/La and Nb/La ratios, and a decrease in Zr/Y, Ce/Y, La/Y and Nb/Y ratios with decreasing silica content. The quartz-plagioclase-porphyry dyke shows similar values to those of the high-silica (67.62%) granodiorite (which gives different values to the other four granodiorites) and possibly represents the extreme case of fractionation. A large body of quartz-feldspar-porphyry from the south-west Rouen Mountains has similar modal compositions to the dyke on Rothschild Island and it is thought to represent the final phase in emplacement of the Rouen Mountains batholith (Care, in press).

The two pre-plutonic hornblende-andesite dykes show similar ratios to those of the average granodiorite, as might be expected if they represent the Elgar Uplands volcanic sequence of northern Alexander Island, which is probably cogenetic with the plutonic rocks of the Rouen Mountains batholith (Care, in press). The ratio for the one analysed intermediate dyke, which is presumed to be post-plutonic from field observations, falls between the average granodiorite and tonalite values for all but the Nb/Y and Nb/La ratios, and is different from the values obtained for the hornblende-andesite dykes. Although these similarities imply a genetic relationship between the plutonic and hypabyssal rocks, it is clear from the variations in major oxide contents that the magma was at a different stage of differentiation when the plutons were emplaced to when the dykes were intruded.

The order of intrusion as deduced from field observations is shown in Table I and is the same as the order of increasing modified Larsen factor $[(\frac{1}{3}Si+K)-(Mg+Ca)]$ with the exception of the intermediate dyke which falls between the hornblende-andesite dykes and the tonalite. A more complicated picture is obtained if the ratios K/Rb, Ba/Rb, Ca/Sr and Zr/Ti are compared (Table IV). All of these ratios should normally decrease upon fractionation (Taylor, 1965; Gill, 1970) as the various elements become depleted within the magma due to preferential partitioning into different minerals. However, as the values in Table IV show, there appears to

TABLE IV. CHEMICAL ANALYSES OF PLUTONIC AND HYPABYSSAL ROCKS FROM ROTHSCHILD ISLAND

	1	2	3	4	5	6	7	8	9	10
SiO_2	67.62	64.65	62.65	62.29	61.57	58.45	71.65	58.91	57.40	55.96
TiO_2	0.41	0.56	0.66	0.58	0.65	0.69	0.23	0.62	0.64	0.75
Al_2O_3	15.33	15.08	15.01	15.72	15.71	15.17	14.54	14.18	15.47	15.57
Fe_2O_3*	3.58	4.54	5.17	5.34	5.67	5.71	1.91	7.58	8.80	8.69
MgO	1.81	1.95	2.56	2.72	2.98	3.54	0.48	6.24	5.57	5.71
CaO	4.04	4.27	5.32	5.84	5.56	6.79	1.59	5.74	6.67	7.75
Na_2O	3.34	3.29	3.52	3.17	3.32	3.29	4.08	2.96	2.14	2.57
K_2O	3.51	3.34	3.90	2.72	2.81	3.40	4.09	2.37	0.90	1.83
H_2O+	0.77	0.66	0.77	0.64	0.72	0.49	0.59	1.82	2.66	1.76
H_2O-	0.40	0.32	0.33	0.50	0.69	0.48	0.64	0.70	0.50	0.59
P_2O_5	0.08	0.14	0.11	0.18	0.15	0.13	0.06	0.12	0.15	0.20
TOTAL	100.89	98.80	99.00	99.70	99.62	98.14	99.86	101.24	100.90	[illegible]38
					ANALYSES LESS TOTAL WATER (RECALCULATED TO 100)					
SiO_2	67.81	66.10	64.00	63.20	62.69	60.15	72.65	59.67	58.73	56.50
TiO_2	0.41	0.57	0.67	0.59	0.66	0.71	0.23	0.63	0.65	0.76
Al_2O_3	15.37	15.42	15.34	15.94	16.00	15.61	14.74	14.36	15.84	15.72
Fe_2O_3*	3.59	4.64	5.28	5.42	5.78	5.88	1.93	7.68	9.00	8.77
MgO	1.82	1.99	2.61	2.76	3.03	3.64	0.49	6.33	5.70	5.77
CaO	4.05	4.37	5.43	5.93	5.56	6.99	1.61	5.81	6.82	7.83
Na_2O	3.35	3.36	3.60	3.22	3.32	3.39	4.14	3.00	2.19	2.60
K_2O	3.52	3.41	2.96	2.76	2.81	3.50	4.15	2.40	0.92	1.85
P_2O_5	0.08	0.14	0.11	0.18	0.15	0.13	0.06	0.12	0.15	0.20
					ELEMENT PERCENTAGES					
Si^{4+}	31.70	30.90	29.92	29.55	29.31	28.12	33.96	27.90	27.46	26.41
Ti^{4+}	0.25	0.34	0.40	0.35	0.40	0.43	0.14	0.38	0.39	[illegible]46
Al^{3+}	8.13	8.16	8.12	8.44	8.47	8.26	7.80	7.60	8.38	8.32
Fe^{3+}†	2.51	3.25	3.70	3.79	4.05	4.12	1.35	5.38	6.30	6.14
Mg^{2+}	1.10	1.20	1.57	1.66	1.83	2.19	0.30	3.82	3.44	3.48
Ca^{2+}	2.89	3.12	3.88	4.24	3.97	4.50	1.15	4.15	4.87	5.60
Na^{+}	2.48	2.49	2.67	2.39	2.46	2.51	3.07	2.22	1.62	1.93
K^{+}	2.93	2.84	2.47	2.30	2.34	2.92	3.46	2.00	0.77	1.54
P^{5+}	0.03	0.06	0.05	0.08	0.06	0.06	0.03	0.05	0.06	0.08
O^{2-}	47.98	47.64	47.22	47.20	47.11	46.89	48.74	46.50	46.71	46.04
Position $[(\frac{1}{3}Si+K)-(Ca+Mg)]$	+9.51	+8.82	+6.99	+6.25	+6.31	+5.60	+13.33	+3.33	+1.61	+1.26

Table IV—*continued*

	1	2	3	4	5	6	7	8	9	10
Alk	59.98	54.50	49.38	46.25	44.94	46.25	79.82	31.45	19.70	26.51
Fe‡	27.83	33.23	35.54	37.38	37.93	35.09	16.50	40.09	51.94	46.91
Mg	12.19	12.27	15.08	16.37	17.13	18.66	3.67	28.46	28.36	26.59
Ca	34.82	36.92	43.02	47.48	45.37	45.32	14.97	49.59	67.08	61.74
Na	29.88	29.46	29.60	26.76	28.05	25.27	39.97	26.52	22.31	21.28
K	35.30	33.62	27.38	25.76	26.68	29.41	45.05	23.89	10.61	16.98
					TRACE ELEMENTS (ppm)					
Ni	5	3	10	5	7	16	—	14	6	8
Cr§	20	20	40	20	30	40	<5	70	10	20
Ce	43	38	44	47	44	32	54	33	41	41
La	23	17	18	21	17	12	27	13	15	16
Zr	128	173	187	147	167	161	136	162	141	130
Nb	6	5	6	4	4	4	7	5	5	3
Y	15	22	29	23	23	28	17	24	20	23
Sr	263	288	307	392	372	400	187	457	490	446
Rb	90	94	79	82	77	96	118	54	30	49
Th	12	12	10	11	9	6	18	5	5	6
Pb	8	12	4	8	6	7	14	25	303	9
W	546	478	503	380	355	221	672	151	93	89
Ga	16	21	18	19	20	21	17	19	21	20
Zn	25	37	9	44	31	36	18	160	442	68
Ba	629	613	505	540	494	347	786	498	198	506
K/Rb	325.56	302.13	312.66	280.49	303.90	304.17	293.22	370.37	256.67	314.29
Ba/Rb	6.99	6.52	6.39	6.59	6.42	3.61	6.66	9.22	6.60	10.33
Ca/Sr	109.89	108.33	126.38	108.16	106.72	112.50	61.50	90.81	99.39	125.56
$Zr \times 10^3/Ti$	51.20	50.88	46.75	42.00	41.75	37.44	97.14	42.63	36.15	28.26

— Below detection limit.
* Total iron as Fe_2O_3.
† Total iron as Fe^{3+}.
‡ Total iron as Fe^{2+}.
§ Values rounded to nearest 10 ppm (not corrected for V interference).

1. KG.2312.5 Granodiorite; northern Rothschild Island.
2. KG.2317.4 Granodiorite; northern Rothschild Island (average of two analyses).
3. KG.2321.4 Granodiorite; western Rothschild Island.
4. KG.2359.8 Granodiorite; southern Rothschild Island.
5. KG.2291.6 Granodiorite; central Rothschild Island.
6. KG.2324.1 Tonalite; western Rothschild Island.
7. KG.2333.1 Quartz-plagioclase-porphyry dyke; central Rothschild Island.
8. KG.2331.5 Intermediate dyke; central Rothschild Island.
9. KG.2343.7 Hornblende-andesite dyke; southern Rothschild Island.
10. KG.2335.3 Hornblende-andesite dyke; central Rothschild Island.

(All analyses by X-ray fluorescence spectrometer at the Department of Geological Sciences, University of Birmingham.)

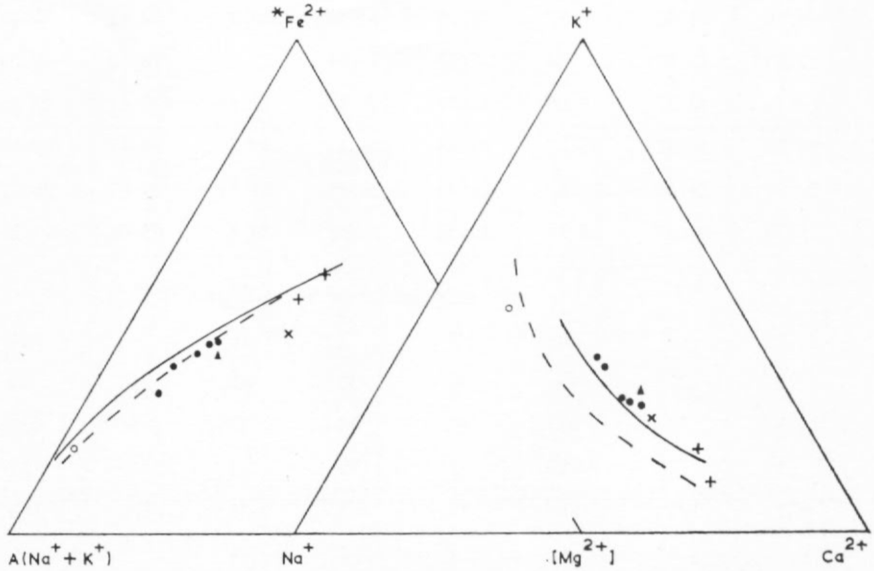

Fig. 9. Triangular A–F–M and Ca–Na–K diagrams for the plutonic and hypabyssal rocks from Rothschild Island. The dashed line is the trend for the Mount Lassen suite (Nockolds and Allen, 1953) and the solid line is the trend determined by Adie (1955) for the Andean Intrusive Suite of Graham Land. ○ quartz-plagioclase-porphyry; ● granodiorite; ▲ tonalite; × intermediate dyke; + hornblende-andesite dykes; $*Fe^{2+}$ is total iron as Fe^{2+}.

TABLE V. COMPARISON OF INTER-ELEMENT RATIOS FOR THE PLUTONIC AND HYPABYSSAL ROCKS FROM ROTHSCHILD ISLAND

	High-SiO_2 granodiorite	*Granodiorite (average of four analyses)*	*Tonalite*	*Quartz-plagioclase-porphyry dyke*	*Intermediate dyke*	*Hornblende-andesite dyke (average of two analyses)*
Zr/Y	8.53	6.99	5.75	8.00	6.75	6.35
Zr/La	5.57	9.35	13.42	5.04	12.46	8.77
Ce/Y	3.07	1.80	1.14	3.18	1.38	1.92
La/Y	1.53	0.76	0.43	1.59	0.54	0.73
Nb/Y	0.40	0.20	0.14	0.41	0.21	0.19
Nb/La	0.26	0.26	0.33	0.26	0.38	0.26

be little consistency in the order among either the plutonic rocks or the hypabyssal intrusions. This is probably due to the small number of analyses available for the area and a better overall picture should be obtained when analyses from the whole of Alexander Island are compared.

Plots of K_2O against SiO_2 content for the major plutonic rocks are compared with similar acid and intermediate rocks from elsewhere in the Antarctic Peninsula in Fig. 10. The rocks from Rothschild Island and Alexander Island have a higher potash content than rocks from adjacent Palmer Land at the same latitude to the east (Davies, 1976; Singleton, 1976; Smith, 1977), although this may be due to an insufficiency of available data. Values are also markedly higher than those from Anvers Island (Hooper, 1962) and the Danco Coast (West, 1974) of Graham Land. Saunders and others (in press) have compared the potash contents of rocks

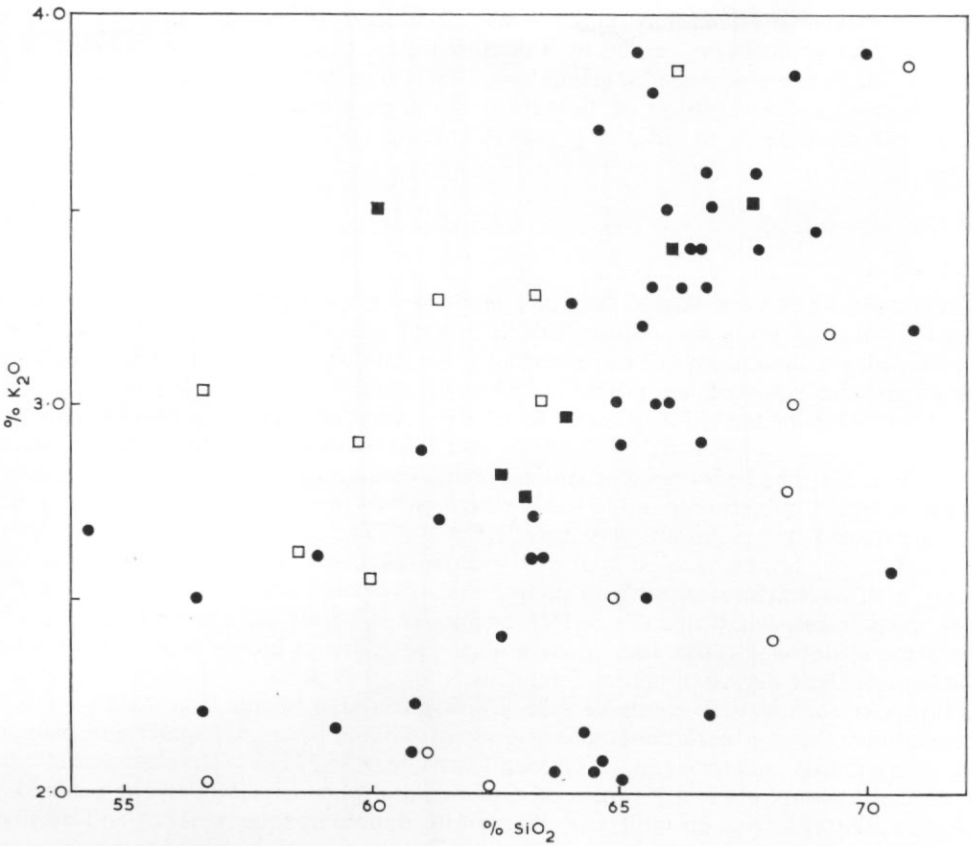

Fig. 10. Plot of K_2O against SiO_2 for some acid and intermediate plutonic rocks from the Antarctic Peninsula.
■ Rothschild Island (this paper).
□ Alexander Island (Care, unpublished data).
● Palmer Land (Davies, 1976, table X; Singleton, 1976, tables III and IV; Smith, 1977, table XXII).
○ West coast of Graham Land (Hooper, 1962, table X; West, 1974, tables V and XI).

from Graham Land and have shown that those from the east coast have a generally higher K_2O content than those from the west coast (which includes the Danco Coast and Anvers Island). They concluded that these differences are consistent with subduction beneath the Antarctic Peninsula from the western (Pacific) side and that radiometric dating shows a trenchward migration of magmatic foci with time and a corresponding decrease in K_2O content.

In Palmer Land, however, K_2O values are broadly comparable or slightly higher than those obtained for the east coast of Graham Land by Saunders and others (in press), and show a slight increase westward into Alexander Island, which is the most westerly site of plutonic activity in the Antarctic Peninsula in terms of distance from the axis of the peninsula. Major plutonic rocks from King George Island in the South Shetland Islands, which lie off the north-west coast of Graham Land and have geographical and geological similarities with Alexander Island (Care, in press), also possess high K_2O values (personal communication from J. L. Smellie).

The significance of this apparent reversal in the general east–west decrease of K_2O content across the Antarctic Peninsula is as yet not understood. The higher potash values for Rothschild

Island and Alexander Island may reflect an increased depth to the Benioff Zone, "K-h variation" (e.g. Dickinson, 1975), caused by a discrete westward stepping of the subduction zone to the far side of accreted material (Hamilton, 1969), or may be simply due to complications arising during the fractionation of different parental magmas with different K_2O and SiO_2 contents and crystallizing in different phases (Cawthorn, 1977).

Cenozoic Volcanic Rocks

Pyroclastic rocks

Poorly consolidated coarse and fine tuffs, lapillistones and lapilli-tuffs (nomenclature after Fisher (1961)) crop out in the south-east of the island, where they form a 100 m cliff face and two rounded, predominantly scree-covered hills. No contacts with other rock formations are observed and the exposures are probably fault-controlled.

The lower 25 m of the cliff exposure (KG.2361) consist of irregularly bedded, pale yellow and brown, coarse and fine palagonite-tuffs and lapillistones possessing a crude columnar jointing (Fig. 11). The beds are cross-laminated and commonly from 2 to 10 cm in thickness, although several 1 m beds crop out in the northern part of the exposure. Patchy, white surface encrustations of (?) gypsum are widespread (Fig. 11). The tuffs comprise a highly variable content of black, brown, orange and grey hyalobasalt clasts, from 2 mm to 5 cm across, together with conspicuous crystals of olivine and pyroxene enclosed in a fine-grained pale brown groundmass. Small nodules of ferromagnesian minerals are contained within several of the black hyalobasalt clasts. Individual laminae are yellow or brown depending on whether the content of these dark scoriaceous fragments is low or high.

In thin section, the tuffs comprise pale yellow-green shards and hyalobasalt clasts with occasional deep brown-black clasts and crystals of olivine, pyroxene, spinel and plagioclase (An_{33-54}) in a matrix of zeolite and, exceptionally, calcite (KG.2361.6). The clasts are invariably vesicular and contain abundant subhedral and euhedral phenocrysts of strongly zoned, pale purple titaniferous augite, enstatite and olivine with minute opaque minerals and plagioclase microlites in a clear isotropic glass, in which the microlites are often aligned to give a trachytic texture. Alteration of the glass to deep orange-yellow palagonite has occurred both in patches throughout the clasts, especially those in the less porous finer-grained tuffs, and as narrow rims to the larger clasts; some of the glass shards are completely altered to palagonite.

Overlying these pale yellow-brown tuffs is a lenticular horizon of dark grey lapilli-tuffs and pale grey coarse tuffs, having a maximum thickness of 30 m, which is vertically down-faulted against the underlying tuffs at the northern end of the exposure. Individual beds vary from 2 to 30 cm in thickness and graded bedding is characteristic of the lapilli-tuffs (Fig. 12); no cross-laminar bedding is evident. The lapilli-tuff (KG.2361.3) is composed almost entirely of uncemented dark vesicular hyalobasalt clasts (from 1 mm to 2 cm across) packed with minute opaque granules and individual ferromagnesian crystals up to 1.5 mm in length. Small (1 mm), bright green, platey and filiform malachite, sometimes with cores of red-brown (?) copper oxide or (?) native copper, is present in some of the interstices.

The paler grey beds of coarse tuff contain pale grey hyalobasalt clasts but few black clasts, and their weaker resistance to erosion than the lapilli-tuffs produces much scree. The volcanic glass of the clasts has been altered to a turbid, brown, slightly pleochroic, microcrystalline clay mineral (?) smectite; cores of unaltered clear glass with patches of palagonite are occasionally seen. Individual crystals are rare and phenocrysts in the clasts are unaltered.

The top of the cliff exposure comprises lapillistones and coarse palagonite-tuffs with an average dip of 25° to the east. They have a similar composition to those tuffs at the base of the succession but with much larger clasts of hyalobasalt (some reaching 25 cm across) and small fragments of a leucocratic fine-grained igneous rock exposed on the bedding planes.

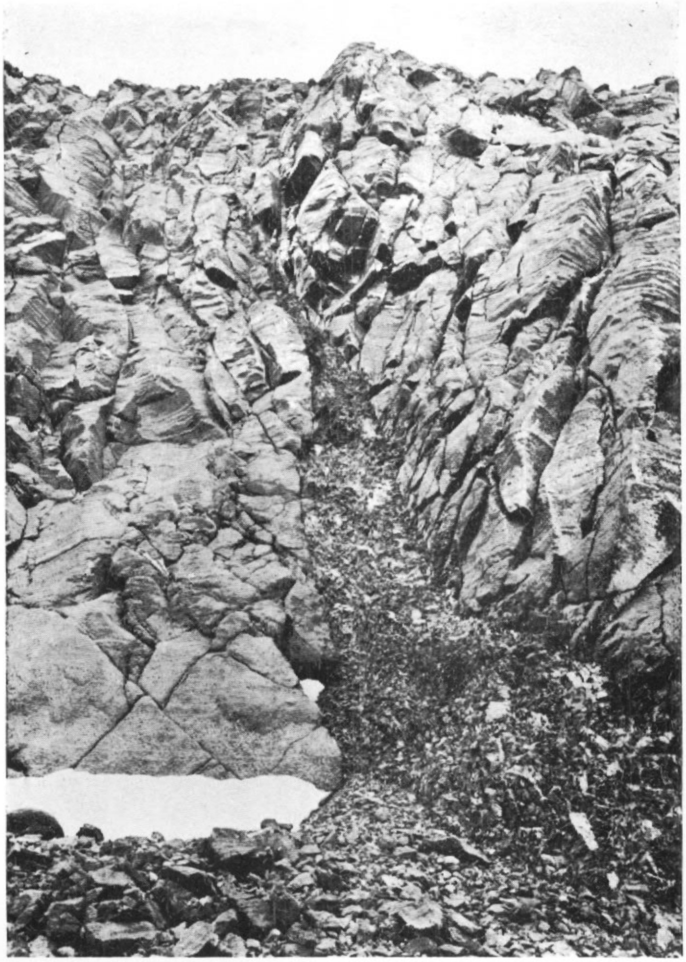

Fig. 11. A highly jointed olivine-basalt dyke intruding palagonite-tuffs in south-east Rothschild Island. The tuffs possess a crude columnar jointing. The maximum width of the dyke is 1.5 m.

The rounded hill exposure (KG.2363) is composed of similar yellow and brown palagonite-lapilli-tuffs, which have a general northerly dip of 18° and display abundant cross laminations, wash-out channels and small-scale faulting (Fig. 13). The outcrop is capped by black scoriaceous scree but no *in situ* exposures are present.

Olivine-basalt dykes

Two near-vertical, rubbly jointed, olivine-basalt dykes intrude palagonite-tuffs in the cliff section at station KG.2361 (Fig. 11). The larger dyke is 1.5 m wide but both pinch out upwards (one within the yellow-brown tuffs, the other reaching the dark grey lapilli-tuffs), indicating that injection was relatively passive. These extremely fine-grained dykes carry rare nodules of ferromagnesian minerals and zones of vesicles flattened parallel to the dyke walls. The basalt is hypocrystalline, comprising phenocrysts of forsteritic olivine up to 1 mm, smaller subhedral labradorite laths with some alteration to sericite, and subhedral, commonly zoned, titaniferous augite in a pale brown-green glass containing olivine, clinopyroxene, plagioclase, granular and

Fig. 12. Graded bedding in a weathered block of lapilli-tuff from the Cenozoic volcanic outcrop in south-east Rothschild Island. The hammer shaft is 35 cm long.

acicular iron ore (Table III). Subhedral phenocrysts of orthopyroxene (enstatite) are uncommon and rare corroded quartz xenocrysts display reaction rims of augite and chlorite. Vesicles are bordered by thin rims of brown glass containing iron-ore microlites.

On the north side of the hill exposure (KG.2363), a composite dyke of olivine-basalt forms a zone of prominent outcrops exceeding 50 m in width with bands of vesicles parallel to the dyke walls. Two types of xenolithic material, often reaching 10 cm across, are common at this locality; rounded crystalline nodules of green ferromagnesian minerals and angular fragments of tonalite with a saccharoidal texture.

The nodules have a lherzolite composition, comprising a coarse interlocking aggregate of forsteritic olivine, colourless clinopyroxene (? diopside), enstatite and small amounts of green spinel (pleonaste). Glide twinning is present in one large enstatite crystal and alteration to iddingsite and antigorite has occurred along some fractures within the olivine. Many of the clinopyroxenes possess highly fractured rims and augite, at the margins of the nodule in contact with the enclosing lava, is zoned outwards to pale purple titanaugite. The tonalite

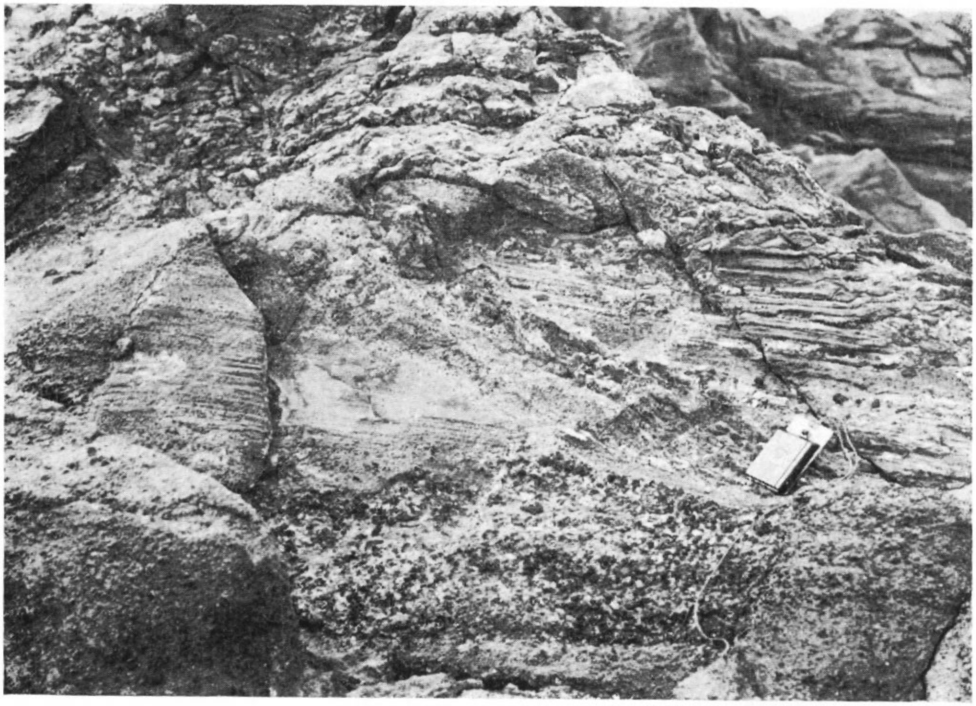

Fig. 13. Cross bedding and minor faulting in lapilli-tuffs, south-east Rothschild Island. The compass is 11 cm long.

xenolith (KG.2363.3; analysis 17 in Table III) displays a much-fractured, hypidiomorphic granular texture with strongly zoned andesine, quartz and rare orthoclase containing abundant small bubble inclusions. Biotite and hornblende are almost completely altered to opaque iron-ore granules.

The hyaloclastite deposits on Rothschild Island are undoubtedly of subaqueous derivation because of their cross bedding, graded bedding and well-sorted nature. It is not possible, however, to determine whether they are of submarine or subglacial origin, although the absence of interbedded marine sediments would favour the latter. Similar rocks are well documented; the James Ross Island Volcanic Group exposed in north-east Graham Land (Nelson, 1975); the Beethoven Peninsula volcanic rocks of south-west Alexander Island (Bell, 1973); and the volcanic rocks of Marie Byrd Land (LeMasurier, 1971). The Rothschild Island volcanic rocks closely resemble those forming cliffs on Beethoven Peninsula, although the palagonite-breccias and the subaerially erupted basalt lava flows are absent from the former locality. The abundance of hyalobasalt scree at station KG.2363 could represent the erosion products of a former lava-flow capping, for which the composite dyke may have been a feeder.

By comparison of the Marie Byrd Land volcanic occurrences with the subglacially erupted hyaloclastites of Iceland, LeMasurier (1971) concluded that submarine and subglacial deposits have the same criteria for recognition. The only direct evidence for subglacial eruption in Antarctica is seen in the Jones Mountains (Rutford and others, 1971) where hyaloclastites overlie lenses of tillite and a glacially stiiated bedrock pavement, and in the southern Elgar Uplands, where the young volcanic rocks rest directly on an ice-striated surface of the older (? Cretaceous) Elgar Uplands volcanic sequence (personal communication from R. W. Burn).

STRUCTURAL GEOLOGY

Local deformation has little affected the LeMay Formation sediments on Rothschild Island but the massive and rubbly jointed nature of the majority of the arenaceous sediments makes it difficult to obtain structural measurements. The infrequent, thinly interbedded sequences of sandstone and mudstone afford the best localities for structural interpretation of these sediments.

Bedding planes dip steeply to the north-west and south-east (Fig. 14a), indicating an initial phase of folding with general north-east to south-west axial traces. A poorly developed slaty cleavage within the argillaceous sediments gives irregular orientations (Fig. 14b) and bedding/cleavage intersections define fold axes with steep plunges (54–68°) to the south-west and west

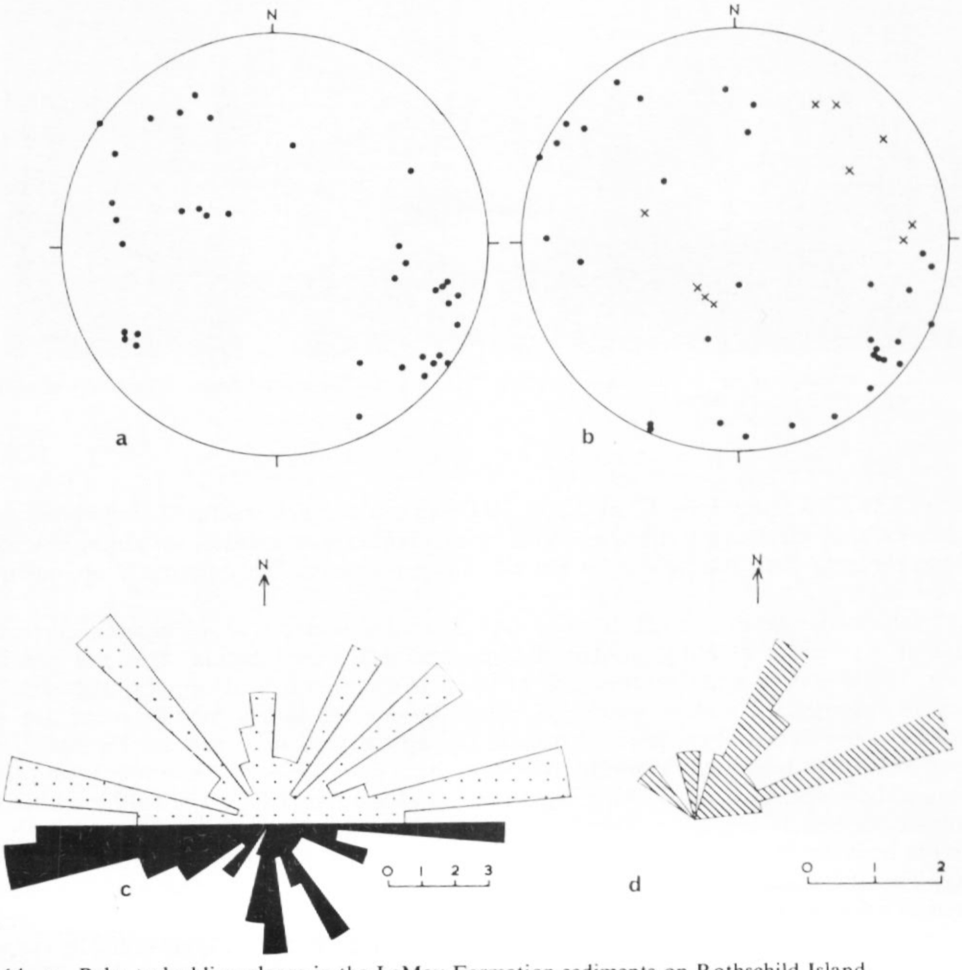

Fig. 14. a. Poles to bedding planes in the LeMay Formation sediments on Rothschild Island.
b. Poles to cleavage planes (●) and bedding/cleavage intersections (×) in the LeMay Formation sediments on Rothschild Island.
c. Orientation of high-angle joint planes (>60°) within the LeMay Formation (stippled) and the major plutonic rocks (hatched) on Rothschild Island. (The number of measurements is indicated in brackets.)
d. Trends of vertical and near-vertical dykes intruding the LeMay Formation. (The number of measurements is indicated in brackets.)

but with only shallow plunges (17–36°) to the north-east and east (Fig. 14b). These suggest a second, possibly asymmetric, period of folding about a general north-west to south-east axis, which could explain the spread of poles to bedding and cleavage in the north-west and south-east quadrants (Fig. 14a and b). No major folds were observed in the field and the axial traces (Fig. 2b) were inferred from the changes in dip of the beds along the various ridges.

The striking west-north-west to east-south-east topographic trend on Rothschild Island is oblique to the main structural trend and is presumably the result of later faulting (possibly strike-slip faulting related to the second phase of folding). Only three major faults were observed in the field: at station KG.2334, where two vertical faults trending 262° and 269° mag. cut the cliff face; and at station KG.2305 (Fig. 4), where a steep northerly dipping fault, trending approximately 100° mag., cuts the headland and can be traced to the east, where it truncates the southern ends of the islands in Lazarev Bay.

The two outcrops of Cenozoic volcanic rocks in the south-east of the island lie on an approximately north-east to south-west line, parallel to the trends of the dykes cutting the exposures. It is interesting to note that outcrops of similar volcanic rock in the southern Elgar Uplands also lie on an approximate north-east to south-west line (personal communication from R. W. Burn), and it appears that fractures with this orientation were sufficiently deep-seated to allow the upward passage of magmatic material in the late Cenozoic.

High-angle joint planes from within the LeMay Formation sediments display a random distribution, whereas the major plutonic intrusions contain joints with a preferred east–west orientation (Fig. 14c). The dominant north-east and east-north-east trends of the dykes within the LeMay Formation (Fig. 14d) show no relationship to the jointing pattern and are probably governed by the strike of the bedding planes.

The predominant north-east to south-west-trending strikes of the LeMay Formation of Rothschild Island differ from those of similar sediments in the adjacent areas of northern Alexander Island to the east, where general north-west to south-east strikes have been recorded from the Havre Mountains (Care, 1977), Nichols Snowfield and south-west Elgar Uplands (personal communication from R. W. Burn). To the west, however, the sediments of Charcot Island have general west-south-west to east-north-east strikes (personal communication from R. W. Burn), similar to those on Rothschild Island. This change in strike direction from east to west across Alexander Island coincides with the belt of cataclastically deformed sedimentary rocks extending north–south through the north-west Havre Mountains, western Nichols Snowfield and into southern Alexander Island, which is thought to have been formed by extensive transcurrent movement deep within the crust (Bell, 1974), and might possibly be related to rotation about this fault zone.

ACKNOWLEDGEMENTS

Thanks are due to my field assistant, R. A. Davies, and to Dr P. D. Clarkson for advice and criticism during the preparation of this paper.

MS received 18 January 1979

REFERENCES

ADIE, R. J. 1955. The petrology of Graham Land: II. The Andean Granite–Gabbro Intrusive Suite. *Falkland Islands Dependencies Survey Scientific Reports*, No. 12, 39 pp.

BELL, C. M. 1973. The geology of Beethoven Peninsula, south-western Alexander Island. *British Antarctic Survey Bulletin*, No. 32, 75–83.

———. 1974. Geological observations in northern Alexander Island. *British Antarctic Survey Bulletin*, No. 39, 35–44.

BLACK, R. B. 1945. Geographical operations from East Base, United States Antarctic Service Expedition, 1939–1941. *Proc. Am. phil. Soc.*, **89**, No. 1, 4–12.

CARE, B. W. 1977. Areas in Alexander Island (Rothschild Island, Havre Mountains and Staccato Peaks) (B.A.S. No. G/1976/R), 10 pp. [Unpublished.]

———. In press. The petrology of the Rouen Mountains, northern Alexander Island. *British Antarctic Survey Bulletin.*

CAWTHORN, R. G. 1977. Petrological aspects of the correlation between potash content of orogenic magmas and earthquake depth. *Mineralog. Mag.*, **41,** No. 318, 173–82.

DALZIEL, I. W. D. *and* D. H. ELLIOT. 1973. The Scotia arc and Antarctic margin. (*In* STEHLI, F. G. *and* A. E. M. NAIRN, *ed. The oceanic basins and their margins. I. The South Atlantic.* New York, Plenum Publishing Corporation, 171–246.)

DAVIES, T. G. 1976. *The geology of part of northern Palmer Land, Antarctica.* Ph.D. thesis, University of Birmingham, 152 pp. [Unpublished.]

DEBENHAM, F., *ed.* 1945. *The voyage of Captain Bellingshausen to the Antarctic seas 1819–1821.* (Translated from the Russian.) London, Hakluyt Society. 2 vols.

DICKINSON, W. R. 1975. Potash–depth (K-h) relations in continental margin and intra-oceanic magmatic arcs. *Geology*, **3,** No. 2, 53–56.

EDWARDS, C. W. In press. Further palaeontological evidence of Triassic sedimentation in western Antarctica. (*In Third Symposium on Antarctic Geology and Geophysics. Madison, Wisconsin, U.S.A., 22–27 August 1977.*)

FISHER, R. V. 1961. Proposed classification of volcaniclastic sediments and rocks. *Bull. geol. Soc. Am.*, **72,** No. 9, 1409–14.

GILL, J. B. 1970. Geochemistry of Viti Levu, Fiji, and its evolution as an island arc. *Contr. Miner. Petrol.* (*Beitr. Miner. Petrogr.*), **27,** No. 3, 179–203.

GRIKUROV, G. E., KRYLOV, A. YA. *and* YU. I. SILIN. 1967. Absolyutnyy vozrast nekotorykh porod dugi Skotiya i Zemli Aleksandra I (Zapadnaya Antarktika) [Absolute age of some rocks from the Scotia arc and Alexander I Land (western Antarctica)]. *Dokl. Akad. Nauk SSSR*, Geology, **172,** No. 1, 168–71. [English translation: *Dokl.* (*Proc.*) *Acad. Sci. U.S.S.R.*, Geological sciences sect., **172,** 19–22.]

HAMILTON, W. 1969. Mesozoic California and the underflow of the Pacific mantle. *Geol. Soc. Am. Bull.*, **80,** No. 12, 2409–30.

HOOPER, P. R. 1962. The petrology of Anvers Island and adjacent islands. *Falkland Islands Dependencies Survey Scientific Reports*, No. 34, 69 pp.

LE MAITRE, R. W. 1976. The chemical variability of some common igneous rocks. *J. Petrology*, **17,** Pt. 4, 589–637.

LEMASURIER, W. E. 1971. Volcanic record of Cenozoic glacial history of Marie Byrd Land. (*In* ADIE, R. J., *ed. Antarctic geology and geophysics.* Oslo, Universitetsforlaget, 251–59.)

———. *and* D. C. REX. In press. Volcanic record of glacial history in Marie Byrd Land and western Ellsworth Land: revised chronology and evaluation of tectonic interrelationships. (*In Third Symposium on Antarctic Geology and Geophysics. Madison, Wisconsin, U.S.A., 22–27 August 1977.*)

NELSON, P. H. H. 1975. The James Ross Island Volcanic Group of north-east Graham Land. *British Antarctic Survey Scientific Reports*, No. 54, 62 pp.

NOCKOLDS, S. R. 1954. Average chemical compositions of some igneous rocks. *Bull. geol. Soc. Am.*, **65,** No. 10, 1007–32.

———. *and* R. ALLEN. 1953. The geochemistry of some igneous rock series. *Geochim. cosmochim. Acta*, **4,** No. 3, 105–42.

PETTIJOHN, F. J., POTTER, P. E. *and* R. SIEVER. 1972. *Sand and sandstone.* New York, Springer-Verlag.

RUTFORD, R. H., CRADDOCK, C., WHITE, C. M. *and* R. L. ARMSTRONG. 1971. Tertiary glaciation in the Jones Mountains. (*In* ADIE, R. J., *ed. Antarctic geology and geophysics.* Oslo, Universitetsforlaget, 239–43.)

SAUNDERS, A. D., WEAVER, S. D. *and* J. TARNEY. In press. The pattern of Antarctic Peninsula plutonism. (*In Third Symposium on Antarctic Geology and Geophysics. Madison, Wisconsin, U.S.A., 22–27 August 1977.*)

SINGLETON, D. C. 1976. *The geology of the central Black Coast, Palmer Land, Antarctica.* Ph.D. thesis, University of Birmingham, 157+25 pp. [Unpublished.]

SMITH, C. G. 1977. *The geology of parts of the west coast of Palmer Land, Antarctica.* Ph.D. thesis, University of Birmingham, 193 pp. [Unpublished.]

TAYLOR, B. J. 1966. *The stratigraphy and palaeontology of the Aptian of the central east coast of Alexander Island.* Ph.D. thesis, University of Birmingham, 245 pp. [Unpublished.]

TAYLOR, S. R. 1965. The application of trace element data to problems in petrology. (*In* AHRENS, L. H., PRESS, F., RUNCORN, S. K. *and* H. C. UREY, *ed. Physics and chemistry of the Earth*, **6.** Oxford, London, Edinburgh, New York, Paris, Frankfurt, Pergamon Press, 133–213.)

THOMSON, M. R. A. *and* R. W. BURN. 1977. Angiosperm fossils from latitude 70°S. *Nature, Lond.*, **269,** No. 5624, 139–41.

WEST, S. M. 1974. The geology of the Danco Coast, Graham Land. *British Antarctic Survey Scientific Reports*, No. 84, 58 pp.